



Wire electrode of 5754 aluminum modified by PVD-thin film depositions

T. Gehling¹ · K. Treutler¹ · V. Wesling¹

Received: 8 August 2022 / Accepted: 29 November 2022 / Published online: 14 January 2023
© The Author(s) 2022

Abstract

Manufacturers of welding wire electrodes for GMAW welding adapt the alloy compositions of welding wire electrodes in order to adjust the weld pool behavior and the properties of the weld. Additively manufactured components in various sizes and with complex structures and multi-axial stress states place diverse demands on the material. The filler wire can significantly influence the material properties. The approach shown here describes the possibility of coating welding wire electrodes by physical vapor deposition, which enables flexible adjustment of the welding material composition. The element content in the weld metal can be adjusted within certain limits via the coating thickness. In the arc, applied thin-film coatings with coating thicknesses $< 1 \mu\text{m}$ pass into the molten phase together with the substrate wire electrode according to ISO 18273—S Al 5754 (AlMg3). Microalloying elements such as TiB_2 or Ti added to the weld pool in this way change the composition and thus influence the microstructure in the weld metal. This results in a grain refinement of up to 46%, which in turn has a positive effect on hot cracking susceptibility. PVD-coated welding electrodes also show changes in arc characteristics. With increasing TiB_2 layer thickness, the arc length decreases by up to 44%, while the arc current increases. The fusion penetration behavior changes from a narrow finger-shaped to a round fusion penetration.

Keywords Welding · Aluminum · Modified welding wire · Grain refinement · Hot cracking reduction · Physical vapor deposition

1 Introduction

The general goal of reducing CO_2 emissions is being pursued in particular with lightweight structures. In the transport and logistics sector in particular, aluminum materials thus offer potential for reducing dead weight and increasing payload. This is, among other things, the reason for the increasing demand in the aluminum sector and goes hand in hand with the requirement that the processing properties of the alloy allow the material to be used in the individual application. In this context, joining technology and, in particular, welding technology play an essential role. Safe joining conditions are requirements for maximum utilization of

the material properties in the subsequent application. The material properties are adapted and specifically influenced by alloying elements. In GMAW welding processes, the chemical composition of the weld metal is influenced in particular by the filler wire. Microalloying elements are added to influence, for example, the mechanical properties or the cracking resistance. The avoidance of hot cracks is a particular challenge in the welding of aluminum materials.

Due to its economic efficiency, the MIG welding process is widely used in the processing of these materials. Various influencing variables have to be considered, which have an influence on the weld seam or the WAAM structure [1]. In addition to the deposition strategy [2] and the travel speed [3], the filler material has a major influence on the resulting material structure. The alloy composition of the filler materials used in this process is adjusted in the molten phase, and the resulting semi-finished products (rod material) are subsequently processed into welding wire electrodes. In addition to the alloy adjustment in the molten phase, cored wires also influence the composition of the weld metal for steel wire electrodes.

Recommended for publication by Commission IX - Behaviour of Metals Subjected to Welding

✉ T. Gehling
tobias.gehling@tu-clausthal.de

¹ Clausthal University of Technology - Institute of Welding and Machining (ISAF), Clausthal-Zellerfeld, Germany

Investigations show that thin-film coatings, which can be applied to selected substrate wire electrodes by PVD processes, are also appropriate for introducing microalloying elements into the weld metal [4–10]. As expected, it is shown that the amount of alloying elements can be modified by adjusting the thickness of the coating. The external coating, however, influences not only the alloy composition and microstructure, but also the welding process.

The grain refining effect of titanium diboride (TiB_2) on various aluminum materials has already been researched [11–14]. In tungsten inert gas welding and laser beam welding, it has been proven that the alloying elements titanium and boron, which are introduced into the welding area by cast inserts, have a corresponding effect [15–20]. By increasing the titanium diboride content with casting inserts in the weld seam area, Schempp [16] was able to reduce the grain size of the alloy AlMg4.5Mn by 44%.

The influence of titanium on the microstructure and grain size has also been investigated [21–25]. Wang, Suo et al. have investigated the influence of titanium powder in the interlayers of a WAAM structure. They note a grain refining effect and increasing tensile strength in the weld metal [26].

The state of research shows that titanium and titanium diboride can have a grain refining effect and influence the microstructure. This effect can be seen both in casting tests and in the welding process, into which the elements are introduced in various ways. In contrast, the possibility of microalloying elements being added to the weld metal of aluminum materials via coatings is not yet widely investigated. The aim of this work is to work out general interactions in the processing of thin-film-coated aluminum welding wire electrodes and their influence on the weld metal and the welding process. The effectiveness of the coatings is to be investigated.

2 Experimental

The tests carried out deal with the GMAW welding process of the aluminum alloy S Al 5754 (AlMg3), according to ISO 18273 [27], which tends to be susceptible to hot cracking. Titanium and titanium diboride (TiB_2) thin-film coatings are to be used to achieve grain refinement of the weld metal structure, which can potentially reduce susceptibility to hot cracking. Furthermore, the coatings influence the arc length, the energy per unit length, and the fusion penetration.

2.1 PVD-coating

For coating the wire electrodes, a PVD system from Ceme-Con AG according to industrial standards is used. Figure 1 shows the coating chamber of the system, which is loaded with the substrate wire electrode in batches.



Fig. 1 PVD coating system with substrate electrode

Table 1 Coating time, resulting layer thickness, and element content

Element	Coating time in min	Coating thickness in nm	Ti in wt.-%
Ti	10	35	0.119
	20	87	0.153
	40	194	0.177
TiB_2	10	31	0.103
	20	47	0.109
	40	129	0.146

Titanium and titanium diboride are applied to the substrate wire electrode in three different layer thicknesses each. Table 1 summarizes the coating thicknesses of the thin-film coatings resulting from the selected coating duration and the titanium content in the weld metal determined by optical emission spectrometry. To determine the coating thicknesses, a half-masked and polished base material sample is added to the respective coating process. After the process, the height difference between the coated and uncoated areas respectively the coating thickness can be measured using a confocal laser scanning microscope. As expected, the coating thickness increases with the coating duration resulting in an increased titanium content in the weld metal.

2.2 Welding and grain size

The coated welding wire electrodes are welded using the parameters summarized in Table 2.

To evaluate the microstructures and in particular to determine the grain size, beads on a plate are welded on substrate material EN AW-5754 according to [28]. The substrate plates are preheated to 100 °C for this purpose. At a length of 70 mm, micrographs are taken from the center of the weld beads, cf. Figure 2.

Table 2 Welding parameters

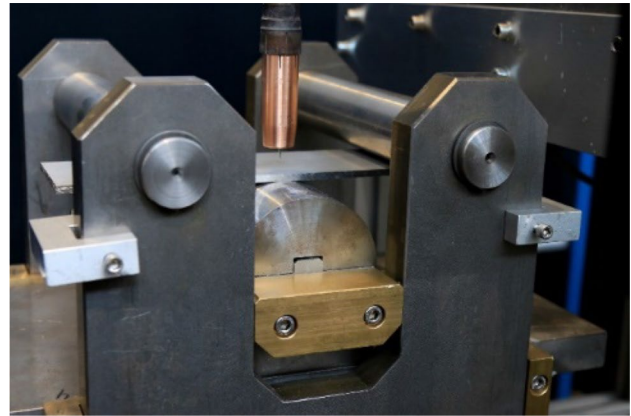
Welding parameters	Value
Wire feed	9.5 m/min
Arc voltage	21.4 V
Welding current	172.6 A
Travel speed	30 cm/min
Energy per unit length	0.73 kJ/mm
Shielding gas	ISO 14175 – II

The weld metal of the uncoated reference wire electrode is shown in comparison with a TiB_2 -coated material. To analyze the microstructures, the microscopic specimens are electrolytically contrasted using the Barker method. For this purpose, the samples are etched 5 times for 40 s at a voltage of 12 V and viewed under polarized light. The influence of TiB_2 on the grain size is evident. To quantify the grain refining effect, five images are taken in each case in the globular dendritically solidified region of the microstructure and then evaluated using the linear intercept method.

2.3 Modified varestraint-transvarestraint test (MVT-test)

To determine the influence of the thin-film coatings on the susceptibility to hot cracking, the modified varestraint-transvarestraint test is carried out in accordance to the DVS code of practice 1004–2 [29] and DIN Technical Report 17,641–3 [30]. In contrast to the test procedure described in that documents, the MIG welding process with a consumable electrode is used.

Figure 3 shows the test setup. For the test, specimens with the dimensions $60 \times 300 \times 10$ mm are inserted into the hydraulic test stand. Starting at the edge of the plate, welding is performed in the direction of the center of the plate using the parameters given in Table 2. The samples are also preheated to 100°C for the MVT test.

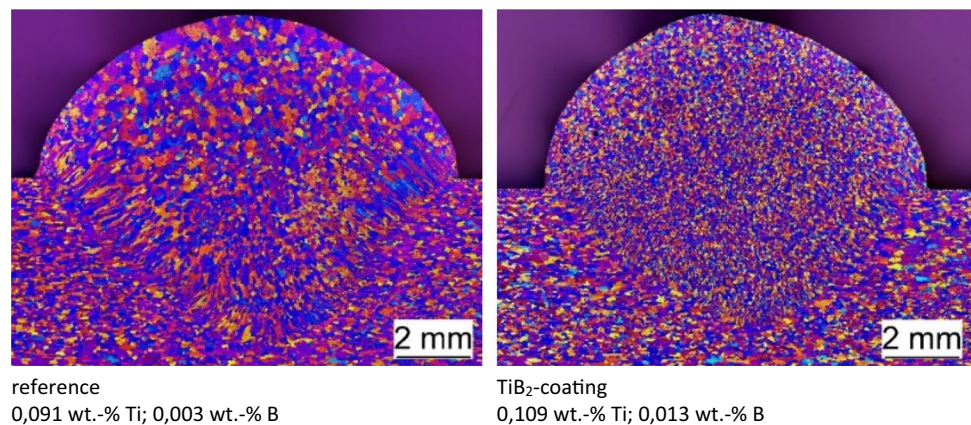
**Fig. 3** Modified varestraint-transvarestraint test

The straining process is triggered at the same time as the torch is switched off in the middle of the substrate plate and the samples are stretched to 1%, 2% and 4% with different matrices. At least 3 specimens are welded for each coating and strain. The weld is then cut out, and the hot-cracked end crater and parts of the weld surfaces on which hot cracks are visible are imaged under a scanning electron microscope. Image analysis software then allows manual measurement of the individual cracks (Fig. 4), which can finally be summed up to a total crack length.

3 Results and discussion

Figure 5 shows the average grain size as a function of the titanium content, for the titanium diboride and for the pure titanium coating.

It gets obvious that the grain size tends to decrease with increasing titanium content in the studied area, in accordance with the theory and in agreement with the research work described further above.

Fig. 2 Comparison of the grain size in the micrograph. Left side, welding wire AlMg3 uncoated. Right side, welding wire AlMg3 with TiB_2 -coatingreference
0,091 wt.-% Ti; 0,003 wt.-% B TiB_2 -coating
0,109 wt.-% Ti; 0,013 wt.-% B

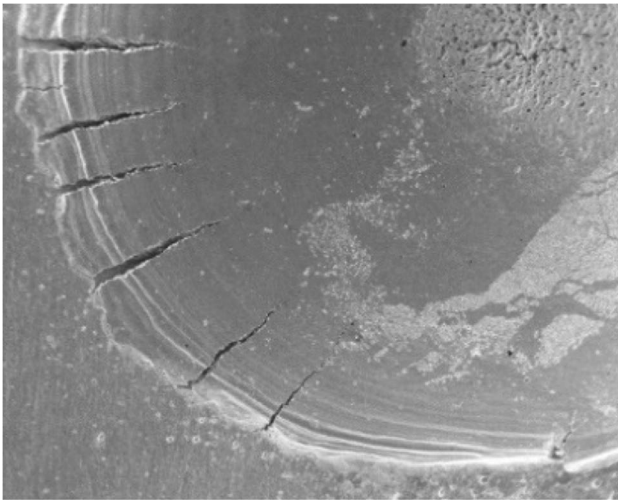


Fig. 4 Hot cracks at the end of a welding seam (SEM)

The results of the modified vareststraint-transvareststraint test are shown in Fig. 6 for titanium and in Fig. 7 for titanium diboride. Both coatings reduce the susceptibility to hot cracking. In particular, the welds with the lowest element contents and thus lowest coating thicknesses lead to the lowest hot cracking susceptibilities compared to the reference.

The influence on the arc is evaluated by high-speed recordings. For this purpose, the substrate plates are moved under the stationary torch with the aid of a robot and the welding speed of the welding process. In this way, high-speed images can be taken at 5000 frames per second over a period of 1 s using the backlight method. In addition, the welding current and the voltage curves of the welding process are recorded simultaneously. To evaluate the high-speed images of the arc, the individual

images of each recording (Fig. 8) are converted into binary images using a thresholding (gray scale) method. The arc length is then measured in the converted images. The angle of the arc is approached at the upper end via the center of the arc 10% below the attachment point at the anode and via the center of gravity of the arc in the two-dimensional image. Figure 9 shows the binary image cropped to the arc. The distance the arc is measured along is shown in red.

To determine the average arc length, the arc lengths of the individual images of the high-speed recording are averaged over the measured period. The changes in arc length in percent compared to the reference arc (uncoated wire electrode) are summarized in Table 3.

It can be demonstrated that the arc length decreases significantly with increasing coating thickness. In the tests carried out, the electrode with the largest TiB_2 layer thickness shows the highest process influence. When the electrode is processed, the arc shortens by 44% compared with the reference. At the same time, the welding current increases by 17% with nearly unchanged arc voltage.

The conductivity of the arc is significantly depending on the degree of ionization and in particular on the metal vapor, since the metallic components in the arc plasma to a large extent carry the arc current. Even traces of metal vapor change the ionization state in the arc column [31]. The coatings can lead to an increase in the metal vapor content and thus to increased electrical conductivity of the arc respectively to a decrease in the length-specific arc resistance. Due to the constant voltage characteristic used in gas metal arc welding, the measured voltage remains nearly constant. The changed operating point of the arc characteristic results in a shorter arc. As the length-specific arc resistance decreases, the welding machine increases the welding current due to the

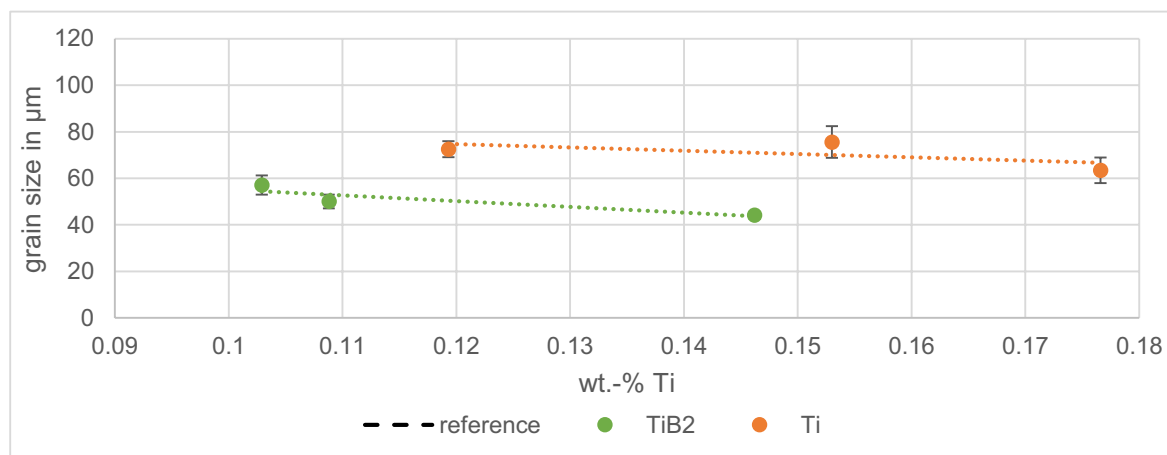


Fig. 5 Grain size as a function of titanium content

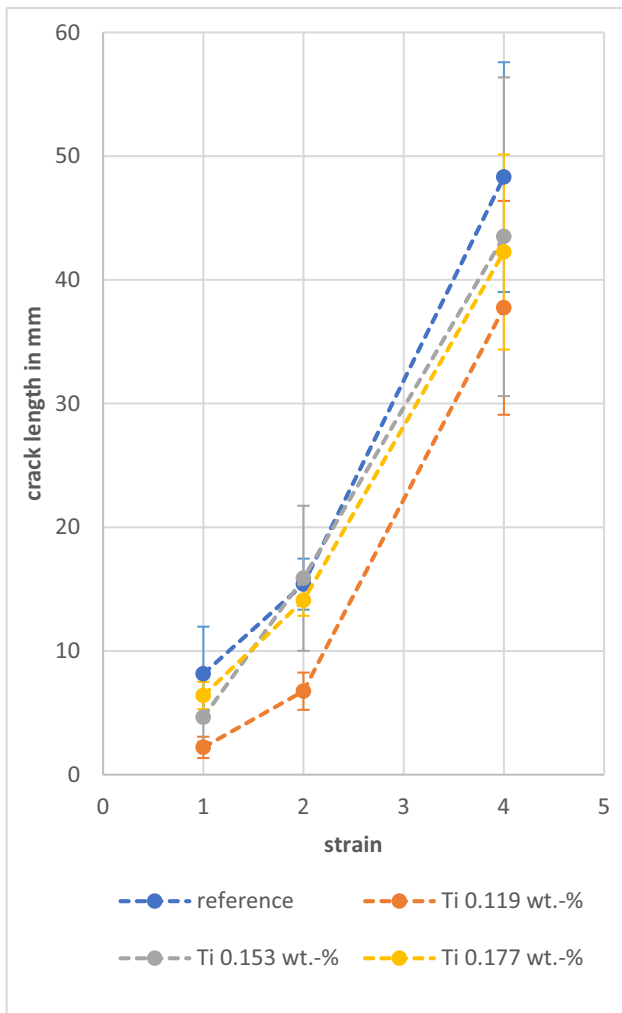


Fig. 6 The result of the trans-varestraint test for Ti-coatings

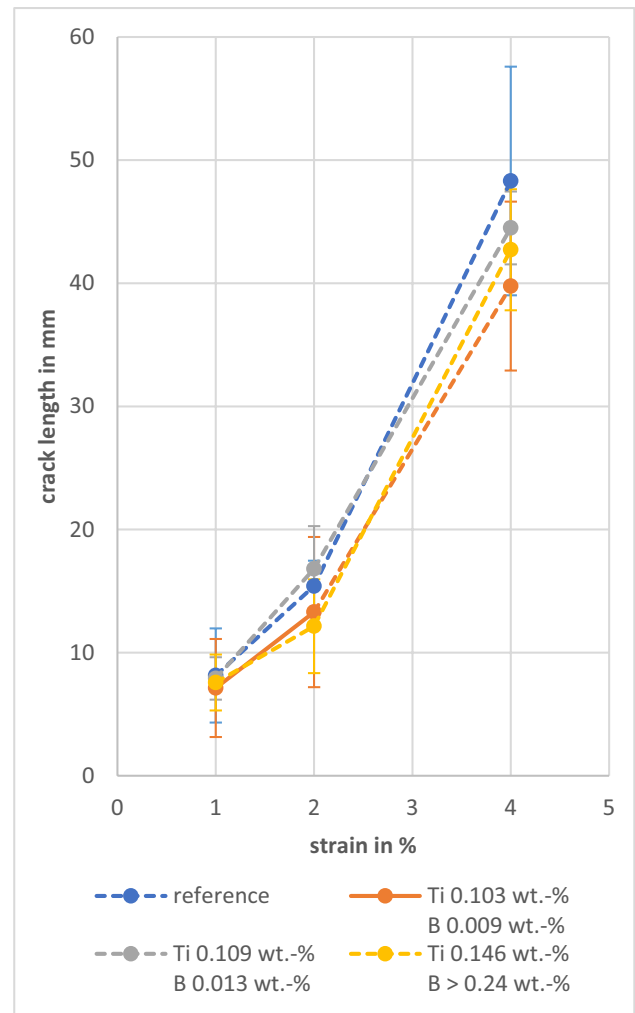


Fig. 7 The result of the trans-varestraint test for TiB₂-coatings

characteristic curve, as also shown by the measurements. Macroscopically, this is manifested by a shorter arc. Figure 10 shows images of the arc with different coatings. The decreasing arc length with increasing coating thickness is visible in the figures.

Another consequence of the increased metal vapor content is the decrease in arc column temperature associated with a wider arc core. The penetration thus becomes flatter and wider. The influence on the fusion penetration shape and the fusion penetration depth of the TiB₂ coatings is clearly shown by micrographs. Figure 11 compares the reference wire electrode with the two higher coating thicknesses. It is noticeable that the penetration decreases with increasing coating thickness and excess weld increases at the same time.

Changes in the penetration shape can be attributed to the fact that the electrically conductive area of the arc expands due to the low ionization energy of the metal vapor and



Fig. 8 The video recording of the welding arc

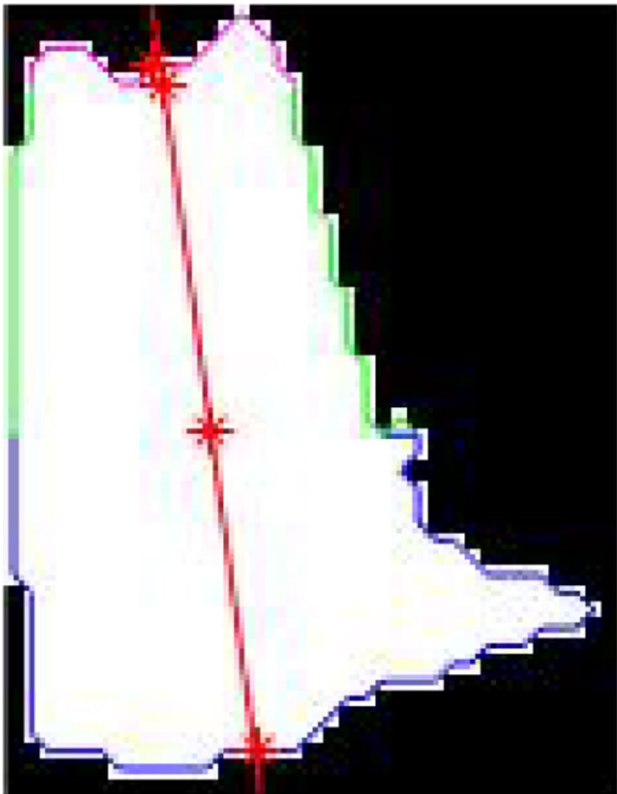


Fig. 9 The binary image of the arc with measuring path

the decreasing current density [32]. It is noticeable that the pore content increases as the TiB_2 content rises. With increasing coating thickness, an increasing hydrogen content in the wire electrodes was observed. However, only very low film thicknesses are required to achieve a significant grain refinement effect, as demonstrated here. Further research is challenged to find the optimum point in terms of film thickness, grain refinement effect, and porosity. In addition, the process parameters of the PVD process can be influenced, possibly leading to a reduction in the hydrogen content of the wire electrodes.

Table 3 Arc length change, welding current, and arc voltage depending on the coating

Coating element	Coating thickness in nm	Ti content in wt.-%	Arc length change in %	Welding current in A	Arc voltage in V
Reference	-	0.091	-	173	21.4
Ti	35	0.119	-18	184	21.3
	87	0.153	-26	191	21.3
	194	0.177	-31	190	21.3
TiB_2	31	0.103	-23	183	21.3
	47	0.109	-31	190	21.3
	129	0.146	-44	202	21.3

4 Conclusions

The investigations carried out show that thin-film coatings can be an interesting tool for influencing the weld metal and the welding process in the welding of aluminum wire electrodes. It was demonstrated that nucleating elements can be introduced into the weld metal via a coating of the filler metals and that a grain-reducing effect can be achieved in this way. By influencing the weld metal and the grain refinement caused by the microalloying elements, the susceptibility to hot cracking can be reduced with a coating of titanium diboride and also with a titanium. In particular, low coating thicknesses show a significant hot crack-reducing effect at high strains. The weld metal with a titanium content of 0.103 wt.% brought in by a titanium diboride coating and the weld metal with a titanium content of 0.119 wt.% brought in by a titanium coating have the lowest hot cracking susceptibility.

In addition, there are clear effects with regard to the welding process, which were illustrated by considering the arc length and the welding process energy. At almost constant arc voltage, the arc length decreases, and the welding current increases with increasing coating thickness. Micrographs show that TiB_2 coatings make the fusion penetration flatter and wider, which can be explained by the influence of the arc plasma via a higher metal vapor content.

Depending on the coating element, high coating thicknesses lead to a correspondingly higher hydrogen input into the welding process and thus to higher porosities in the weld metal. For some elements, however, the coating thicknesses required for positive weld metal and process effects are far below a critical range in terms of hydrogen-induced porosity.

5 Outlook and future research

In addition to titanium and titanium diboride, the effect of other coating elements on the weld metal and the process is worth investigating. It is also worthwhile to extend the investigations to other substrate wire electrodes. The substrate wire electrode chosen here is a naturally hard alloy. Research

Fig. 10 Influence of coatings on the arc length

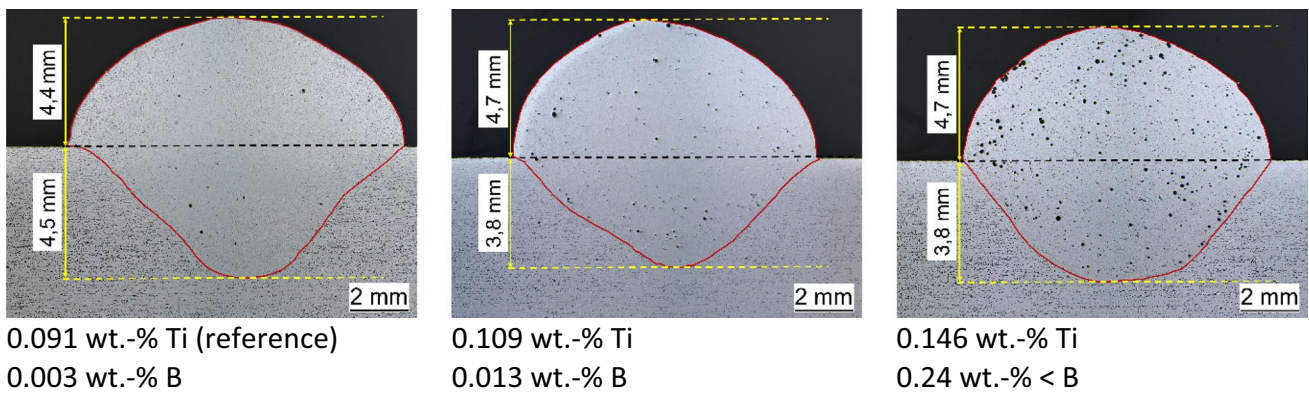
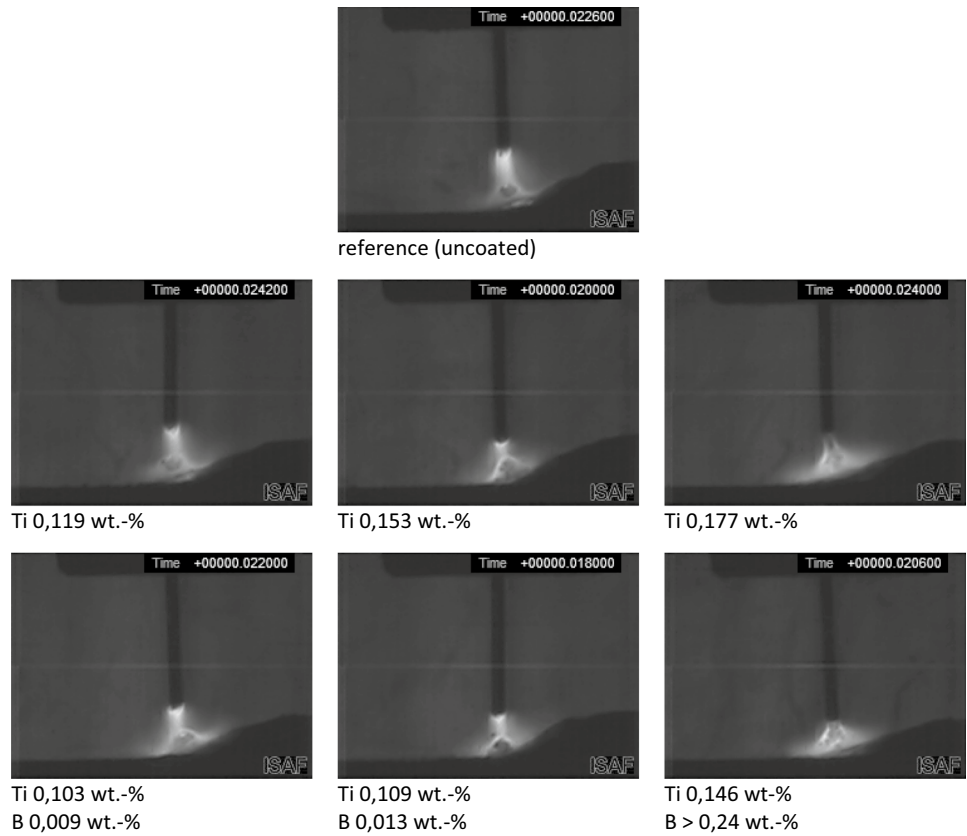


Fig. 11 Fusion penetration and excess weld of the welding seam depending on the TiB₂-coating

should be extended into the area of heat-treatable alloys. Initial results show an influence on the mechanical-technological properties and thus the need for further research in this respect. In terms of the coating process, further investigations can be made to reduce the inherent hydrogen content of the coatings.

Funding Open Access funding enabled and organized by Projekt DEAL. Funded by the Deutsche Forschungsgemeinschaft (DFG, German Research Foundation) – Project-ID 413693695.

Data Availability The datasets generated during the current study are available from the corresponding author on reasonable request.

Declarations

Conflict of interest The authors declare no competing interests.

Open Access This article is licensed under a Creative Commons Attribution 4.0 International License, which permits use, sharing, adaptation, distribution and reproduction in any medium or format, as long as you give appropriate credit to the original author(s) and the source, provide a link to the Creative Commons licence, and indicate if changes were made. The images or other third party material in this article are included in the article's Creative Commons licence, unless indicated otherwise in a credit line to the material. If material is not included in the article's Creative Commons licence and your intended use is not permitted by statutory regulation or exceeds the permitted use, you will need to obtain permission directly from the copyright holder. To view a copy of this licence, visit <http://creativecommons.org/licenses/by/4.0/>.

References

1. Tawfik MM, Nemat-Alla MM, Dewidar MM (2021) Enhancing the properties of aluminum alloys fabricated using wire + arc additive manufacturing technique - a review. *J Mater Res Technol* 13:S. 754–768
2. Su C, Chen X, Kononov S, Arvind Singh R, Jayalakshmi S, Huang L (2021) Effect of deposition strategies on the microstructure and tensile properties of wire arc additive manufactured Al-5Si alloys. *J Mater Eng Perform* 30:S. 2136–2146 (3)
3. Tawfik MM, Nemat-Alla MM, Dewidar MM (2021) Effect of travel speed on the properties of Al-Mg aluminum alloy fabricated by wire arc additive manufacturing. *J Mater Eng Perform* 30:S. 7762–7769 (10)
4. Gehling T, Treutler K, Wesling V (2019) Beeinflussung der Schweißnahtfestigkeit höchstfester Feinkornbaustähle durch beschichtete MSG-Schweißdrahtelektroden. *DVS-Berichte* 356:S. 103–112
5. Gehling T, Treutler K, Wesling V (2019) Dünnfilmbeschichtung von MSG-Schweißdrahtelektroden - Schweißgut- und Prozesseigenschaften. *DVS-Berichte* 357:S. 11–18
6. Gehling T, Treutler K, Wesling V (2019) Targeted influence on the weld strength of high-strength fine-grain structural steels in the GMA welding process through functionalized weld material surfaces. *Weld World* 63:S. 783–792 (3)
7. Gehling T, Treutler K, Wesling V (2019) Assistentenseminar Füge- und Schweißtechnik. Vorträge der gleichnamigen Veranstaltung in Braunlage vom 25. bis 27. September 2019. Dünnfilmbeschichtung von MSG-Schweißdrahtelektroden : Schweißgut- und Prozesseigenschaften. *DVS Berichte*. Düsseldorf: DVS Media 2020
8. Gehling T, Treutler K, Wesling V (2021) Development of surface coatings for high-strength low alloy steel filler wires and their effect on the weld metal microstructure and properties. In: *Weld World*. <https://doi.org/10.1007/s40194-021-01086-3>
9. Treutler K, Schram, Au, Wesling, V (2017) Beeinflussung des MSG-Schweißprozesses und der Eigenschaften des Schweißgutes durch Zusatzelemente auf der Drahtoberfläche // 36. Assistentenseminar Fügetechnik. *DVS-Berichte* 36. Assistentenseminar Füge- und Schweißtechnik // Band 320. Düsseldorf: DVS Media GmbH, S. 27–32
10. Wesling V, Treutler K, Gehling T (2018) Influence on the weld strength of high-strength fine-grained structural steels by thin-film-coated GMA welding electrodes. *IOP Conf Ser: Mater Sci Eng* 373:S. 12006
11. Easton M, StJohn D (1999) Grain refinement of aluminum alloys: Part I. the nucleant and solute paradigms—a review of the literature. *Metall Mater Trans A* 30:S. 1613–1623 (6)
12. Easton M, StJohn D (1999) Grain refinement of aluminum alloys: part II. Confirmation of, and a mechanism for, the solute paradigm. *Metall Mater Trans A* 30:S. 1625–1633 (6)
13. Johnsson M, Backerud L, Sigworth GK (1993) Study of the mechanism of grain refinement of aluminum after additions of Ti- and B-containing master alloys. *Metall Trans* 24:S. 481–491 (2)
14. Khrustalyov AP, Kozulin AA, Zhukov IA, Khmeleva MG, Vorozhtsov AB, Eskin D, Chankitmongkol S, Platov VV, Vasilyev SV (2019) Influence of titanium diboride particle size on structure and mechanical properties of an Al-Mg alloy. *Metals* 9:S. 1030 (10)
15. Schempp P, Cross CE, Schwenk C, Rethmeier M (2012) Influence Of Ti and B additions on grain size and weldability of aluminium alloy 6082. *Weld World* 56:S. 95–104 (9–10)
16. Schempp P (2013) Grain refinement in aluminium GTA welds. *Zugl.: Berlin, Techn. Univ., Diss., 2013. BAM-Dissertationsreihe, Bd. 111. Berlin: Bundesanstalt für Materialforschung und -prüfung (BAM)*
17. Tang Z, Schempp P, Seefeld T, Schwenk C, Vollertsen F (2011) Kornfeinung bei WIG- und Laserstrahlschweißen von Aluminiumlegierungen. In: *Große Schweißtechnische Tagung 2011, Studentenkongress 2011, Abschlusskolloquium Lichtbogen-schweißen 2011. Vorträge der Veranstaltungen im Rahmen von DVS Congress und DVS Expo in Hamburg vom 27. bis 29. September 2011. DVS-Berichte, Bd. 275. Düsseldorf: DVS Media, S. 153–163*
18. Schempp P, Schwenk C, Rethmeier M, Edward C (2011) Weld metal grain refinement of aluminium alloy 5083 through controlled additions of Ti and B. *Mater Test* 53:S. 604–609 (10)
19. Tang Z Heißrisssvermeidung beim Schweißen von Aluminiumlegierungen mit einem Scheibenlaser. *Zugl.: Bremen, Univ., Diss., 2014. Strahltechnik, Bd. 53. Bremen: BIAS 2014*
20. McCartney DG (1989) Grain refining of aluminium and its alloys using inoculants. *Int Mater Rev* 34:247–260 (Nr. 1)
21. Delamore GW, Smith RW (1971) The mechanisms of grain refinement in dilute aluminum alloys. *Metall Trans* 2:S. 1733–1738 (6)
22. Maxwell I, Hellawell A (1975) A simple model for grain refinement during solidification. *Acta Metall* 23:S. 229–237 (2)
23. Sigworth GK, Kuhn TA (2007) Grain refinement of aluminum casting alloys. *Int J Metalcast* 1:S. 31–40 (2)
24. Vinod Kumar GS, Murty BS, Chakraborty M (2010) Effect of TiAl₃ particles size and distribution on their settling and dissolution behaviour in aluminium. *J Mater Sci* 45:S. 2921–2929 (11)
25. Yunjia H, Frost R, Olson D, Edwards G (1989) Grain refinement of aluminum weld metal. Titanium and zirconium microadditions have a strong influence on grain size, solidification rate and nucleation time on grain size, solidification rate and nucleation time. *Weld J* 68:S. 280–289 (7)
26. Wang L, Suo Y, Liang Z, Wang D, Wang Q (2019) Effect of titanium powder on microstructure and mechanical properties of wire + arc additively manufactured Al-Mg alloy. *Mater Lett* 241:S. 231–234
27. DIN EN ISO 18273:2016–05. *Schweißzusätze – Massivdrähte und -stäbe zum Schmelzschweißen von Aluminium und Aluminiumlegierungen – Einteilung*
28. DIN EN 573–3:2019–10. *Aluminium und Aluminiumlegierungen. Chemische Zusammensetzung und Form von Halbzeug - Teil 3: Chemische Zusammensetzung und Erzeugnisformen*
29. Merkblatt DVS 1004–2:2019–10. *Heißrisssprüfverfahren mit fremdbeanspruchten Proben*

30. DIN-Fachbericht 17641–3:2004. *Zerstörende Prüfung von Schweißverbindungen an metallischen Werkstoffen Heißrisprüfungen für Schweißungen – Lichtbogenschweißprozesse . Teil 3: Fremdbeanspruchte Prüfungen*
31. Schellhase M Der Schweißlichtbogen - ein technologisches Werkzeug. Fachbuchreihe Schweisstechnik, Bd. 84. Düsseldorf: Dt. Verl. für Schweisstechnik 1985
32. Murphy AB (2013) Influence of metal vapour on arc temperatures in gas–metal arc welding: convection versus radiation. *J Phys D: Appl Phys* 46:S. 224004 (22)

Publisher's note Springer Nature remains neutral with regard to jurisdictional claims in published maps and institutional affiliations.